# The Effect of Water Column Stability on Acoustic Backscatter from the Ocean Bubble Layer

Kathy K. Bekker, Kenneth E. Gilbert, and Ralph R. Goodman

Applied Research Laboratory and the Graduate Program in Acoustics
The Pennsylvania State University
P.O. Box 30, State College, PA 16804
E-mail: keg5@psu.edu

## Abstract

*This paper investigates the effect of near-surface water column stability on both low-frequency ($f < 5$ kHz) and high-frequency ($f = 248$ kHz) acoustic backscatter from the ocean bubble layer. It is shown that, with the same windspeed but different stability conditions, backscatter strengths can differ by more than an order of magnitude. It is concluded that water column stability is important not only for accurate predictions of total backscatter, but also for understanding the relative contributions of different surface and near-surface scattering mechanisms.*

## 1. Introduction

The initial motivation for the present investigation came from the observation [1] that a good deal of low-frequency backscatter data show levels much lower than estimated by the empirical data fits proposed by Chapman/Harris [2] and Ogden/Erskin [3]. To explain the discrepancies, we have hypothesized that, in addition to wind speed, water column stability plays an important role in determining bubble cloud structure and hence backscatter strengths. Support for the validity of the hypothesis is given by the low-frequency backscatter data of a number of authors [2-6] and by calculations from a theoretical model for low-frequency backscatter [7]. In addition, the upward-looking 248 kHz sonar measurements of Thorpe [8] show directly the effect of water column stability on bubble cloud structure and on high-frequency backscatter. Thorpe's high-frequency backscatter data are used to infer the inputs needed for the low-frequency backscatter calculations which predict a strong dependence on water column stability.

## 2. Water Column Stability and Low-Frequency Backscatter

The backscattering of low-frequency sound from rough, wind driven sea surfaces has been the subject of many studies over the last half century [2-6,9]. The obvious relationship between windspeed and backscattering strength has been consistently observed and has led to the development of useful *empirical* algorithms relating the two quantities, [2,3]. It has been widely noted [1,3,4,10], however, that under similar windspeed conditions, there can be significant differences in backscatter strengths. The differences are large enough and common enough to lead one to conclude that windspeed alone is insufficient as a predictive parameter. In seeking an explanation for the discrepancies, we have found a significant correlation between low-frequency backscatter strength and the air-sea heat flux.

In the present discussion of low-frequency backscatter, we take as a working hypothesis that, at a given windspeed, air-sea heat flux controls the gravitational stability of the near-surface region of the water column (0-10 m), and that water column stability is an important parameter affecting surface backscatter. The hypothesis implicitly assumes that much of the low grazing angle backscatter is due to tenuous microbubble clouds (as opposed to the rough surface or dense near-surface plumes), and that the gravitational stability of the upper water column can strongly affect the distribution of wave-generated microbubbles near the surface, thereby affecting the backscatter.

Although the data available from reported backscatter experiments are insufficient to accurately determine the water column stability that existed during the acoustic measurements, there are some cases in which the environmental conditions allow limited comparisons to be made. We can compare, for example, the gross differences in scattering strength under conditions, which for purposes of discussion, we broadly categorize as "winter" or "summer" conditions. For "winter" conditions we mean specifically that the near-surface water is very well mixed, and the air above it is colder. For "summer" conditions the air is warmer than the sea, and there is sufficient heating to cause a strong temperature gradient .

Winter conditions, as we have defined them, were undoubtedly present during the measurements of Chapman-Harris

[2] and Chapman-Scott [4], as well as during Critical Sea Tests 2, 4, and 6, reported by Ogden and Erskin [3]. On the other hand, summer conditions probably prevailed in the early measurements taken during the FASOR tests [5] in summer in the Western Pacific, in the measurements made during CST 1, 3, and 5 [3], and probably in those of Richter [6] near Nassau in February. The experimental reverberation results, especially above 500 Hz, show markedly different scattering strengths, roughly 10 dB at angles 10° to 20°, with backscatter generally higher in winter conditions than the summer conditions. (See, for example, data reported by Ogden and Erskin [3], Figures 16 and 17, Runs 33A, 28B, 33M)

Although the correlation of low-frequency backscatter with winter/summer conditions is significant, there are cases where it is not evident. One obvious reason for the imperfect correlation is that, in addition to seasonal heat flux, other factors affect stability of the upper water column (e.g., diurnal convective heating and cooling, evaporation, cloud cover, etc.). As a result, the degree of near-surface stability spans a continuum in both winter and summer conditions, so that without measurements of the crucial environmental parameters, we can make only a partial correlation with backscatter. In order to obtain a better understanding of the relation between backscatter and water column stability, we have sought more definitive evidence for the effect. Such evidence can be found by considering high-frequency scattering from the bubble layer, which we discuss next.

## 3. High-Frequency Backscatter Measurements from an Upward-Looking Sonar

Upward-looking high-frequency sonars provide a useful visualization of the structure of the bubble layer as well as a quantitative measure of the high-frequency backscatter [8,11]. Thorpe, for example, in a comprehensive study of bubble clouds, has used sonagraphs from an upward-looking 248 kHz sonar to show clearly the different bubble cloud structures and bubble transport processes that occur in unstable and stable conditions [8]. He has also processed the data to obtain the scattering cross section per unit volume.

Figures 1 and 2 show results from Thorpe's measurements for unstable and stable conditions [8]. In the figures, note that while the average wind speed (bottom panel) is essentially the same for both cases, the bubble cloud structures shown in the sonagraph displays (top panels) are distinctly different. To describe the differences in the bubble cloud structure, Thorpe has coined the terms "columnar clouds" for the structure in the unstable case in Fig. 1 and "billow clouds" in the stable case in Fig. 2. In the unstable situation, heat is flowing from the ocean to the atmosphere so that there is a negative temperature gradient (temperature increases downward) and a positive density gradient (density increases upward). As a result of having denser water over less dense water in the upper water column, downward moving turbulent currents generated by breaking waves continue to move downward producing columnar bubble clouds. Conversely, in stable conditions, the reverse situation exists, with the less dense water over denser water in the upper water column. Because of buoyancy, turbulent currents created by breaking waves do not continue downward but, instead, decay rapidly and form billow clouds, which collectively make a thinner, more homogeneous bubble layer than in unstable conditions.

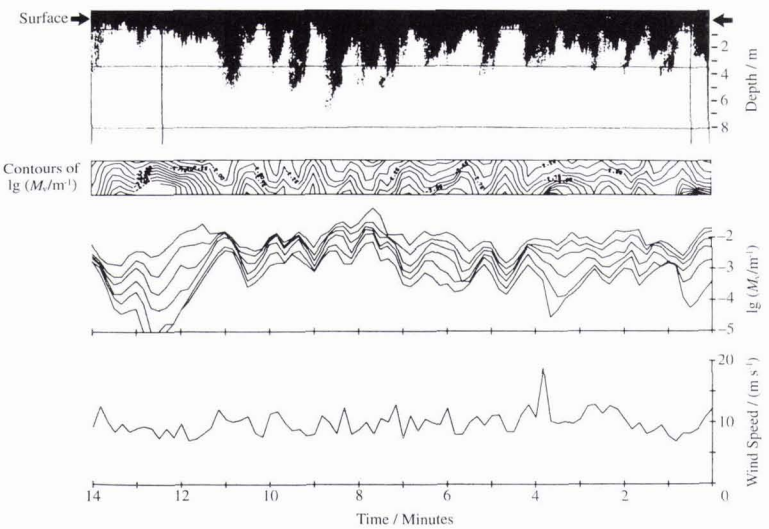


Fig. 1. Backscatter measurements from a 248 kHz upward-looking sonar for unstable conditions (air-sea temperature difference is -1.2°K). First panel: sonagraph records, time increasing to the left. Second panel: contours of $\log_{10}(M_v)$ vs depth and time (contour interval is 0.25). Third panel: values of $\log_{10}(M_v)$ vs time at six equally spaced depths (see description in text). Fourth panel: windspeed vs time. (From S.A. Thorpe [8].)

In Figs. 1 and 2, the second and third panels show the values of scattering strength per unit volume, $M_v$, measured by the upward-looking sonar. The second panel shows contours of $\log_{10}(M_v)$ vs time while the third panel gives the actual values of $\log_{10}(M_v)$ vs time at six depths equally spaced between the top two horizontal lines shown in the figure. The top line, which is not visible in the stable case, is approximately .5 m below the surface (indicated by an arrow). The second horizontal line marks the lower limit of the backscatter sampling region and is located at depths of approximately 3.5 m and 5.5 m, respectively, in the unstable and stable cases. The sampling depth indicated by the third horizontal line, at approximately 8 m, was normally well below the bubble clouds and was used to establish the noise level of the system.

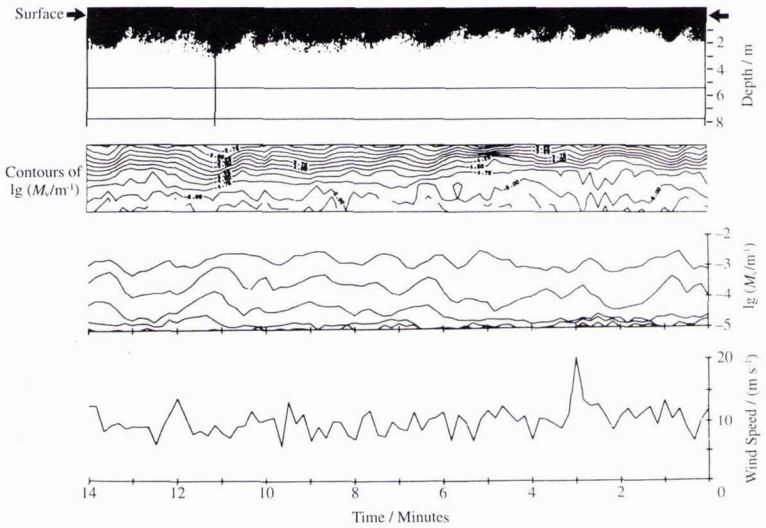


Fig. 2. Same as Fig. 1 except for stable conditions (air-sea temperature difference is +1.3°K). Note that the average windspeed is essentially the same as in Fig. 1, but the bubble-cloud structure is significantly different. (From S.A. Thorpe [8].)

Even a casual inspection of $\log_{10}(M_v)$ vs time in the third panel shows a drastic difference in backscatter in stable conditions compared to unstable conditions. To obtain a quantitative measure of the differences in $M_v$ for unstable and stable conditions, we have digitized the $\log_{10}(M_v)$ vs time curves in the third panel and computed the time average of $M_v$ and its standard deviation vs depth. We find, as did Thorpe in Ref.[8], that the depth dependence of the time average of $M_v$ is well fit by an exponential of the form:

$$\langle M_V(z)\rangle = \langle M_V(0)\rangle e^{-z/\langle L\rangle}, \tag{1}$$

where $\langle M_v(0)\rangle$ is the value at z = 0 (extrapolated exponentially from .5 m), and $\langle L\rangle$ is the e-folding distance. The values we obtained for $\langle M_v(0)\rangle$ for unstable and stable conditions are $2.49 \times 10^{-2}$ m$^{-1}$ and $4.54 \times 10^{-3}$ m$^{-1}$, respectively, a reduction in backscatter of almost a factor of ten in the stable case. The corresponding e-folding distances $\langle L\rangle$ are, respectively, 1.1 m and .7 m. The values we obtained for the exponential parameterization of $\langle M_v(z)\rangle$ are similar to the values reported by Thorpe and show that high-frequency backscatter in stable conditions can differ dramatically from that in unstable conditions.

In addition to computing the mean value, we have used the time series for $M_v$ to compute the standard deviation in $M_v$ vs depth and found it also to be well represented by an exponential:

$$\sigma_{Mv}(z) = \sigma_{Mv}(0)e^{-z/L}, \tag{2}$$

where for unstable and stable conditions, respectively, we obtained $1.96 \times 10^{-2}$ m$^{-1}$ and $6.65 \times 10^{-3}$ m$^{-1}$ for $\sigma_{Mv}(0)$, and 1.4 m and .5 m for the e-folding distance, L. Thus, in stable conditions, the standard deviation, like the mean, is greatly reduced.

The above results for $\langle M_v(z)\rangle$ and $\sigma_{Mv}(z)$ make it clear that both the mean and variance in high-frequency backscatter can be significantly less in stable conditions than in unstable conditions. The difference in the mean backscatter in the two situations implies not just a difference in bubble cloud structure (columnar clouds versus billow clouds) but, in addition, a much smaller density of bubbles in the billow bubble clouds that form in stable conditions. Thorpe [8] has hypothesized that in stable conditions there are fewer bubbles because wave breaking is reduced due to the gravitationally stable atmosphere that is coincident with the gravitationally stable ocean in summer conditions. It seems unlikely, however,

that wave breaking would be decreased by a factor of ten in even in very stable conditions. Consequently, the greatly reduced bubble density in stable conditions must be regarded at present as an unexplained phenomenon. Regardless of the physical mechanisms responsible for reducing the bubble density, it appears that in stable conditions, high-frequency backscatter can be systematically lower than in unstable conditions by as much as 10 dB.

## 4. Theoretical Analysis For Low-Frequency Backscatter

In this section we return to the issue of low-frequency backscatter. We seek to estimate the differences in low-frequency scattering strength one might expect at a fixed windspeed for unstable conditions (columnar clouds) and stable conditions (billow clouds). To do so, we use a low-frequency scattering model that depends on the statistics of the sound speed fluctuations in the bubble layer. Measurements of the sound speed fluctuations, which result from the stochastic distribution of bubbles in the bubble layer, are not presently available at a fixed windspeed for unstable and stable conditions. Consequently, it is necessary to infer the inputs needed for the low-frequency calculations from the high-frequency upward-looking sonar measurements in the previous section.

### 4.1 Backscatter Model

The theoretical model that we use for backscatter is a coherent backscatter model applicable to low-frequency (non-resonant), low grazing angle backscatter [7]. The essential input needed for the model is the variance (or standard deviation) in sound speed as a function of depth in the bubble layer. The theoretical model assumes that the standard deviation in sound speed versus depth can be fitted with an exponential of the form:

$$\sigma_c(z) = \sigma_c(0)e^{-z/L}, \tag{3}$$

where $\sigma_c(0)$ is the near-surface standard deviation, and L is the e-folding distance. We show below that $\sigma_c(z)$ is proportional to $\sigma_{Mv}(z)$, which itself decays exponentially with depth. Hence, at this point, the assumed exponential form is at least plausible. The exponential decay with depth has, in fact, been observed in in-situ measurements [11,12,13] and is a physically realistic representation of actual sound speed fluctuations.

With the coherent backscatter model of Ref. [7], the scattering cross section per unit area, $\Sigma_{scat}$, is given by

$$\Sigma_{scat} = [3/(4\pi c_o^2)][\sigma_c^2(0)L][k_o^4 S(-2k_h)]\left[\frac{4k_v^4L^4}{(1+4k_v^2L^2)(1+k_v^2L^2)}\right], \tag{4}$$

where $c_o$ is the sound speed in bubble-free water, $k_o = \omega/c_o$ is the corresponding wavenumber, $k_h = k_o\cos\theta$ is the horizontal wavenumber, and $k_v = k_o\sin\theta$ is the vertical wavenumber. The normalized wavenumber spectrum for sound speed fluctuations, S(q), is taken to be Von Karman's interpolation formula for inertial subrange (Kolmogorov) turbulence [14],

$$S(q) = 0.35\frac{8\pi^{3/2}}{K_o^3}(1+q^2/K_o^2)^{-11/6}. \tag{5}$$

The parameter $K_o$ is $2\pi/L_o$, where $L_o$ is the outer scale of turbulence and is taken to be the mixed layer depth. For the sake of simplicity, the inner scale of turbulence is taken to be zero.

For wavelengths significantly smaller than the bubble layer thickness L, we have $\lambda/L << 1$, and $k_vL >> 1$, so that the fourth bracket in (4) is nearly unity. Hence, in the short wavelength limit, the ratio of the scattering cross sections for unstable and stable conditions is

$$\frac{\Sigma_{scat}(\text{unstable})}{\Sigma_{scat}(\text{stable})} \xrightarrow{\lambda/L \to 0} \frac{[\sigma_c^2(0)L]_{unstable}}{[\sigma_c^2(0)L]_{stable}}. \tag{6}$$

Thus, for non-resonant scattering, the crucial scaling parameter is $\sigma_c^2(0)L$, which can be thought of as the depth-integrated variance in sound speed. As described below, we can use Thorpe's high-frequency upward-looking sonar data to estimate the variance in sound speed as a function of depth.

### 4.2 Estimates for $\sigma_c(z)$

To get values for $\sigma_c(0)$ and L, and hence $\sigma_c(z)$, we make use of the time series measured by Thorpe for the high-frequency scattering per unit volume, $M_v$, at various depths in the bubble layer. To use $M_v$ for this purpose, we first need to establish

the connection between $M_v$ and the sound speed reduction in the bubble layer. We can then show that the standard deviation in sound speed is proportional to the standard deviation in $M_v$.

For low frequencies and low void fractions in tenuous microbubble clouds, the fractional sound speed reduction due to the presence of bubbles can be written as [15]

$$\Delta c(\mathbf{r},t)/c_0 = 8{,}200\ \phi(\mathbf{r},t)\ , \tag{7}$$

where $\phi(\mathbf{r},t)$ is the void fraction and $c_0$ is the speed of sound in bubble-free sea water. To proceed further, we need at this point to obtain a relation between $\phi(\mathbf{r},t)$ and $M_v(\mathbf{r},t)$.

Under the assumption of dominance by single scattering, we can write $M_v(\mathbf{r},t)$ as

$$M_V(\mathbf{r},t) = \int_0^\infty \Sigma_{bub}(\omega,a)N(\mathbf{r},a,t)da\ , \tag{8}$$

where $\Sigma_{bub}(\omega,a)$ is the scattering cross section at angular frequency $\omega$ for a single bubble of radius a. The quantity $N(\mathbf{r},a,t)da$ gives the number of bubbles per unit volume with radii between a and a + da as a function of space and time. With the assumption that the statistics of the bubble distribution scale with the number density but are otherwise stationary, we can approximate the bubble distribution as

$$N(\mathbf{r},a,t) \equiv N_0(\mathbf{r},t)\eta(a)\ , \tag{9}$$

where $N_0(\mathbf{r},t)$ is the space-time distribution for the total number of bubbles per unit volume, and $\eta(a)$ is the size distribution. We define the integral of $\eta(a)$ to be unity. The approximation in (9) is reasonable at depths far enough below the wave breaking region that the bubble cloud has had sufficient time to lose the larger bubbles and only the smaller bubbles ($a < 200\ \mu$) remain. Hence we can evaluate the integral in (8) as

$$M_V(\mathbf{r},t) = N_0(\mathbf{r},t)\int_0^\infty \Sigma_{bub}(\omega,a)\eta(a)da\ , \tag{10}$$

For a fixed frequency, the integral in (10) is a constant. Thus is clear that if (9) holds, then $M_V(\mathbf{r},t)$ is proportional to the total number of bubbles per unit volume:

$$M_V(\mathbf{r},t) = N_0(\mathbf{r},t)<\Sigma_{bub}(\omega)>\ , \tag{11}$$

where $<\Sigma_{bub}(\omega)>$ is the bubble-size averaged cross section resulting from the integral in (10).

The void fraction can be written in terms of the number of bubbles per unit volume and the average bubble volume:

$$\phi(\mathbf{r},t) = N_0(\mathbf{r},t)< v >\ , \tag{12}$$

where the average bubble volume $< v >$ is given by

$$< v > = \frac{4}{3}\pi\int_0^\infty a^3\eta(a)da\ . \tag{13}$$

Hence the void fraction $\phi(\mathbf{r},t)$ is proportional to the scattering cross section per unit volume $M_v(\mathbf{r},t)$,

$$\phi(\mathbf{r},t) = \left[\frac{< v >}{<\Sigma_{bub}(\omega)>}\right] M_V(\mathbf{r},t)\ . \tag{14}$$

Since the reduction in sound speed $\Delta c$ is proportional to $M_v$, the sound speed itself can be written as

$$c(\mathbf{r},t) = c_0 - \gamma M_V(\mathbf{r},t)\ , \tag{15}$$

where the constant of proportionality $\gamma$ is given by

$$\gamma = 8{,}200\left[\frac{< v > c_0}{<\Sigma_{bub}(\omega)>}\right]\ . \tag{16}$$

The standard deviation in sound speed is hence proportional to the standard deviation in $M_v$:

$$\sigma_c(z) = \gamma\,\sigma_{M_V}(z)\ . \tag{17}$$

To determine the constant of proportionality, $\gamma$, we could assume some bubble distribution model and calculate the quantities in (16). However, since we are mainly interested in comparing backscatter in unstable and stable conditions, we simply adjust $\gamma$ to obtain agreement with measured low-frequency backscatter for unstable conditions. Then, having the proportionality constant, we can make predictions for the stable situation. For typical backscatter in unstable conditions and a windspeed of 25 kts, the constant of proportionality was found to be $\gamma = 9.13 \times 10^3$. To give some idea of the values of sound speed reduction $\Delta c$ that are associated with variations in $M_V$ in unstable and stable conditions, in Fig. 3 we show both quantities versus time and at $z = 0$ (extrapolated exponentially from .5 m). The values obtained for $\sigma_c(z = 0)$ are 179 m/s and 61 m/s, respectively, for unstable and stable conditions. The associated e-folding distances are, of course, the same as obtained earlier for $\sigma_{Mv}(z)$, i.e., L = 1.4 m in unstable conditions and L = .5 m in stable conditions.

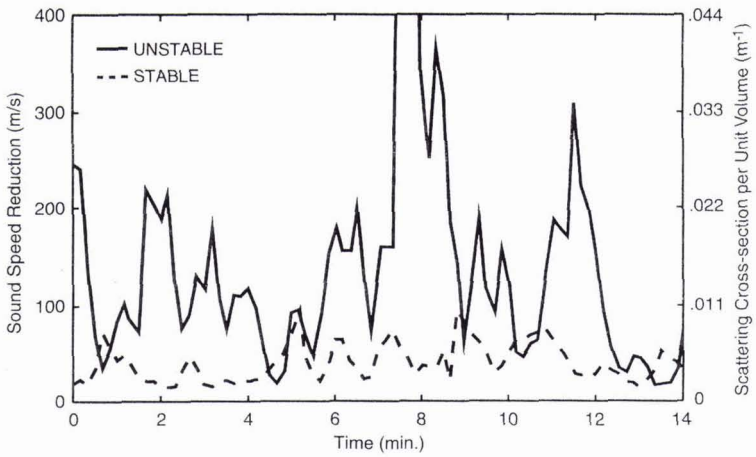


Fig. 3. Sound speed reduction and scattering strength per unit volume vs time for unstable conditions (solid line) and stable conditions (dashed line). The curves shown are values extrapolated exponentially to zero depth from the first sampling bin at approximately .5 m depth.

### 4.3 Predictions for Low-Frequency Backscatter

The above estimates for $\sigma_c(z)$, together with $\Sigma_{scat}$ in (4), were used to make predictions for low-frequency backscatter from the ocean bubble layer in unstable and stable conditions. In the predictions shown in Figs. 4 and 5, scattering strength is defined as $10\log_{10}(\Sigma_{scat})$, and the outer scale $L_O$ is taken to be 106 m, a value that is realistic in high sea states [16].

Figure 4 shows the predicted scattering strength vs grazing angle at several frequencies for unstable and stable conditions. The dashed lines are the backscatter for bubble layer scattering only. The lower curve (marked with x's) is for stable conditions and is essentially just a downward displaced (20 to 30 dB) version of the upper curve (marked with o's), which is for unstable conditions. As they stand, the unstable/stable curves for bubble layer scattering bear little resemblance to the winter/summer measurements of Ogden and Erskin, which generally differ by no more than 5 to 10 dB between winter and summer conditions and are not simply displaced versions of each other. The probable reason for the discrepancy is that other scattering mechanisms, such as rough surface scattering, are present. When scattering from the bubble layer drops below a certain level, other scattering mechanisms dominate the backscatter so that the backscatter level does not drop precipitously and, in addition, can have a different grazing angle dependence. To account approximately for rough surface scattering, and hence better represent the backscatter levels actually measured in stable conditions, we have added incoherently the rough surface scattering contribution from the perturbation model of Thorsos [17]. The backscatter results for the bubble layer plus rough surface scatter are the solid lines, with the o's and x's indicating unstable and stable conditions, respectively. The addition of a rough surface scattering contribution has little effect for unstable conditions but noticeably raises the backscatter levels in stable conditions. The net result is to capture the trends found in the data of Ogden and Erskin for winter and summer conditions (e.g., runs 28B and 33A). For example, in both the data and the predictions, the difference between unstable and stable conditions is larger at higher frequencies than at lower frequencies. Also, both data and predictions show that the effect of water column stability is larger at smaller grazing angles than at larger grazing angles. The predicted difference between winter/summer conditions (i.e., unstable/stable conditions) is 10 to 20 dB and hence is about twice the measured values. Nevertheless, the predicted trends with frequency and grazing angle are consistent with the data. Hence the theoretical predictions, together with the backscatter data, support the water column stability hypothesis. In addition, in the analysis of data, the theory helps to identify the relative contributions of scattering

from the microbubble layer and from other scattering mechanisms such as the rough surface and dense, near-surface plumes.

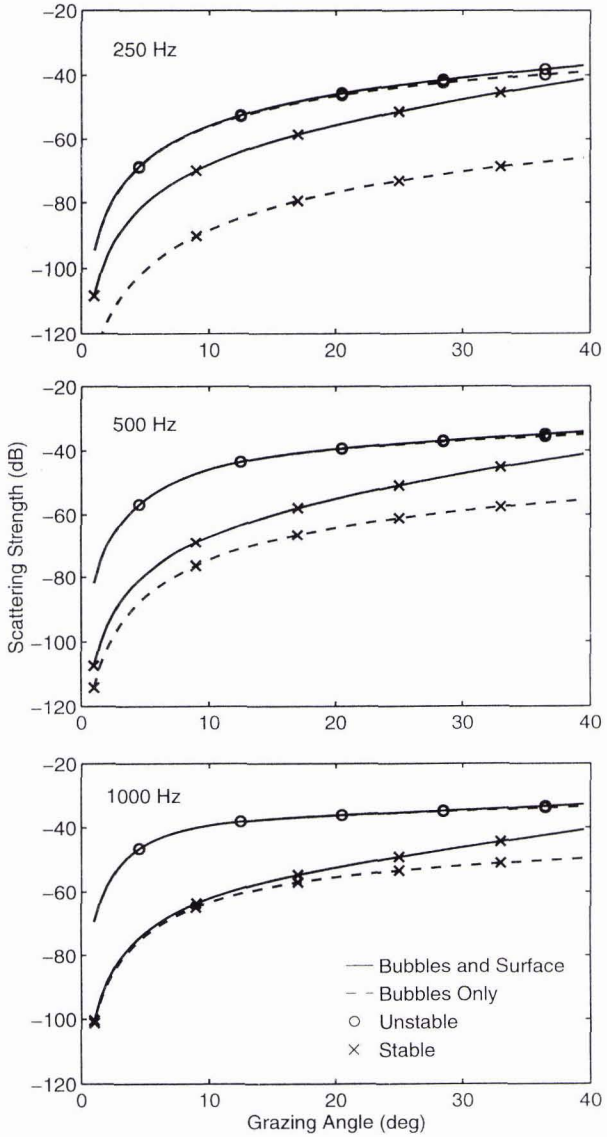


Fig. 4. Scattering strength vs grazing angle at several fixed frequencies. The circles and triangles are for unstable and stable conditions, respectively. The dashed lines denote backscatter just from the bubble layer. The solid line denotes the incoherent sum of bubble layer scattering and rough surface scattering.

Figure 5 shows scattering strength vs frequency at several fixed grazing angles. Although, in principle, Fig. 5 contains the same information as Fig. 4, the display of backscatter vs frequency shows more clearly the differences between backscatter in unstable and stable conditions. In Fig. 5, as in Fig. 4, without rough surface scatter the curves for stable conditions have the same shape as for unstable conditions but are displaced by 20 to 30 dB. With the inclusion of a rough surface contribution, however, the backscatter in stable conditions never drops below the rough surface scattering "floor" which has its own characteristic frequency dependence. As a result, the frequency dependence below 500 Hz is quite different in stable conditions from that in unstable conditions. The obvious difference in the frequency dependence should provide a useful way to sort out the different physical mechanisms that contribute to the observed total backscatter.

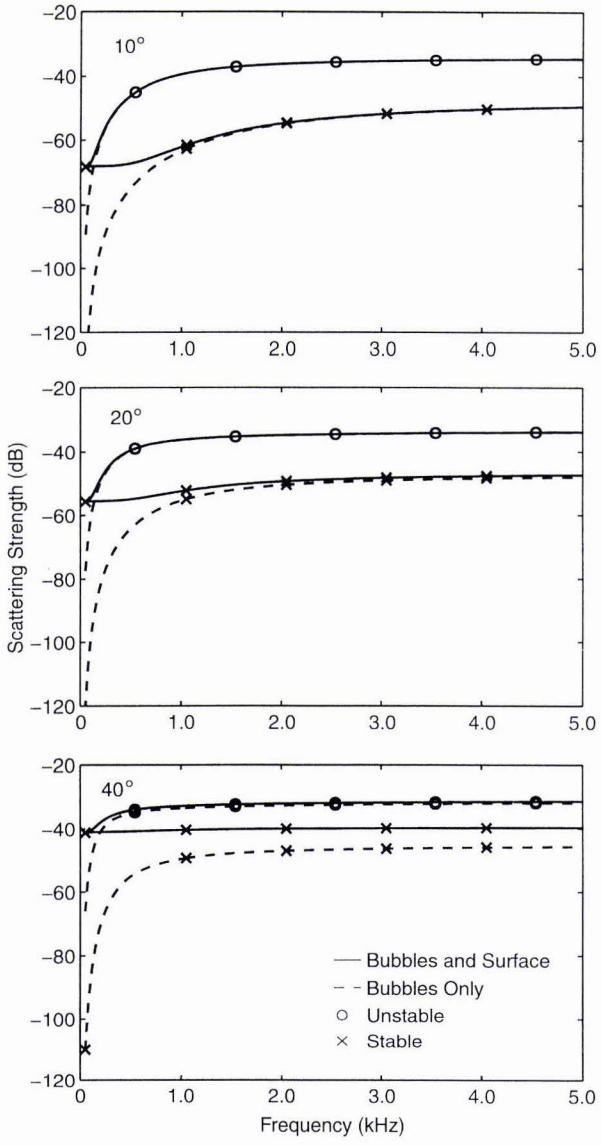


Fig. 5. Same as Fig. 4, except that the grazing angles are fixed and the frequency is varied.

## 5. Summary and Conclusions

We have presented experimental and theoretical evidence that the stability of the near-surface water column significantly affects both low-frequency and high-frequency backscatter from the ocean bubble layer. At low frequencies, the evidence was essentially circumstantial. However, at 248 kHz, the evidence from the upward-looking sonar measurements of Thorpe was direct and clear-cut. There seems to be little question that bubble cloud structure and high-frequency backscatter can vary dramatically with water column stability.

From the calculations of low-frequency backscatter, it was shown that analysis of backscatter in unstable and stable conditions can help to identify the relative contributions of different scattering mechanisms. In particular, if future low-frequency backscatter data show a marked dependence of backscatter on water column stability, it will point to microbubble clouds (as opposed to the rough sea surface or dense, near-surface plumes) as the primary low-frequency scattering mechanism.

Finally we point out that existing empirical expressions for low-frequency backscatter [2,3] apply to unstable conditions. Consequently, if stable conditions are found to occur frequently, it will be important to incorporate water column stability as a parameter in predictive operational models for low-frequency backscatter. Similarly, for reliable predictions in both unstable and stable conditions, high-frequency operational models should also include the effects of near-surface water column stability.

## Acknowledgments

The authors are grateful for support from the Office of Naval Research. The first author (KKB) was supported under the Augmentation Awards for Science and Engineering Research Training (AASERT) program. The other authors (KEG and RRG) received partial support from the Ocean Acoustics Program (Code 321OA).

## References

[1] R. R. Goodman, "A critique on the relationship between backscattering and environmental measurements," 123rd meeting of the Acoustical Society of America, Salt Lake City, May 11-15, 1992.

[2] R.P. Chapman and J.H. Harris, "Surface backscattering strengths measured with explosive sources," J. Acoust. Soc. Am., vol. 34, pp. 1592-1597, 1962.

[3] P.M. Ogden and F.T. Erskin, "Surface scattering measurements using broadband explosive charges in the Critical Sea Test experiments," J. Acoust. Soc. Am., vol. 95, pp. 746-761, 1993.

[4] R.P. Chapman and H.D. Scott, "Surface backscattering strengths measured over an extended range of frequencies and grazing angles," J. Acoust. Soc. Am., vol. 36, pp. 1735-1737, 1964.

[5] J.L. Percy, "Surface backscattering strengths from several FASOR II deep-water stations," Naval Undersea Research and Development Center Technical Publication NUC TP 185, 1970.

[6] R.M. Richter, "Measurements of backscattering from the sea surface," J. Acoust. Soc. Am., vol. 36, pp. 864-869, 1964.

[7] K.E. Gilbert, "A stochastic model for scattering from the near-surface oceanic bubble layer," J. Acoust. Soc. Am., vol. 94, pp. 3325-3334, 1993.

[8] S.A. Thorpe, "On the clouds of bubbles formed by breaking windwaves in deep water, and their role in air-sea gas transfer," Philos. Trans. R. Soc. London, Ser. A, vol. 304, pp. 155-210, 1982.

[9] J.R. Brown, J.A. Scrimger, and R.G. Turner, "Reverberation from the ocean surface," Pacific Naval Laboratory, Esquimalt, B.C., Canada, Technical Memorandum 66-8, 1966.

[10] S.T. McDaniel, "Sea surface reverberation: A review," J. Acoust. Soc. Am., vol. 94, pp. 1905-1922, 1993.

[11] D.M. Farmer and S. Vagle, "Waveguide propagation of ambient sound in the ocean surface bubble layer," J. Acoust. Soc. Am., vol. 86, pp. 1897-1908, 1989.

[12] E. Lamarre and W.K. Melville, "Sound-speed measurements near the ocean surface," J. Acoust. Soc. Am., vol. 96, pp. 3605-3616, 1994.

[13] M.Y. Su, personal communication, 1992.

[14] S.F. Clifford, "The Classical Theory of Wave Propagation in a Turbulent Medium," in *Laser Beam Propagation in the Atmosphere*, edited by J.W. Strohbehn (Springer-Verlag, New York, 1978).

[15] R.J. Urick, *Principles of Underwater Sound*, (McGraw-Hill, New York, 1975), 2nd ed., p. 224.

[16] D.M. Farmer, Cruise Report, CSS John P. Tully, 17 February to 6 March 1992, Institute of Ocean Sciences, Sidney, B.C., Canada.

[17] E.I. Thorsos, "Acoustic scattering from a 'Pierson-Moskowitz' sea surface," J. Acoust. Soc. Am., vol. 88, pp. 335-349, 1990.